

MARCH 01 2007

## Vortex sound due to a flexible boundary backed by a cavity in a low Mach number mean flow

S. K. Tang; R. C. K. Leung; R. M. C. So



*J. Acoust. Soc. Am.* 121, 1345–1352 (2007)

<https://doi.org/10.1121/1.2434240>



### Articles You May Be Interested In

Acoustic radiation by vortex induced flexible wall vibration

*J. Acoust. Soc. Am.* (October 2005)

A computational study of the interaction noise from a small axial-flow fan

*J. Acoust. Soc. Am.* (September 2007)

Vortex sound in the presence of a low Mach number flow across a drum-like silencer

*J. Acoust. Soc. Am.* (May 2011)



LEARN MORE

Advance your science and career as a member of the  
**Acoustical Society of America**

# Vortex sound due to a flexible boundary backed by a cavity in a low Mach number mean flow

S. K. Tang<sup>a)</sup>

*Department of Building Services Engineering, The Hong Kong Polytechnic University, Hong Kong, China*

R. C. K. Leung and R. M. C. So

*Department of Mechanical Engineering, The Hong Kong Polytechnic University, Hong Kong, China*

(Received 26 April 2006; revised 5 November 2006; accepted 15 December 2006)

Low frequency sound radiated due to the unsteady motion of an inviscid vortex in the proximity of a flexible membrane backed by an airtight cavity on an otherwise rigid plane is investigated theoretically. Results show that both monopole and dipole are created but the latter is important only when the vortex is traversing over the membrane. The monopole results from the membrane vibration and the dipole from the transverse motion of the vortex. It is also found that these sound fields tend to counteract each other. The increase in the mean flow speed in general results in a stronger acoustic power radiation, but sound attenuation may be possible if the membrane-cavity system is weak compared with the mean flow momentum. © 2007 Acoustical Society of America. [DOI: 10.1121/1.2434240]

PACS number(s): 43.28.Ra, 43.40.Rj, 43.50.Nm [GCL]

Pages: 1345–1352

## I. INTRODUCTION

It is well known that the unsteady motion of turbulence is an important source of aerodynamic sound, especially in the presence of nonrigid solid surfaces.<sup>1,2</sup> The regeneration noise inside and the breakout noise from an air duct in a building conveying low Mach number turbulent flow are typical examples of such sound.<sup>3</sup> Silencing devices, such as the dissipative silencer and expansion chamber,<sup>4</sup> which are adopted to attenuate fan noise in the ventilation system will also interact with the turbulent flow to produce noise. This low frequency aerodynamic noise is relatively difficult to attenuate in a cost-effective manner.

It has been confirmed that the low Mach number flow tends to amplify the low frequency aerodynamic sound power radiation (for instance, Ffowcs Williams and Lovely,<sup>5</sup> Dowling,<sup>6</sup> and Howe<sup>7</sup>). It also produces a Doppler effect which alters the directivity of the sound radiation. Recently, Huang<sup>8</sup> has shown that a flexible membrane backed by a cavity inside a rigid walled duct can result in significant sound attenuation in the absence of a mean flow. In the presence of a turbulent flow, the unsteady motions of the turbulence and the flow-induced membrane vibration are expected to be sound producing and thus will deteriorate the performance of the membrane setup of Huang.<sup>8</sup> In fact, the self-noise generated by various duct silencing devices in the presence of turbulent flow is one of the very hot research topics.

Direct computation of sound generated by a low Mach number flow is difficult enough because of the great disparity in scales between the acoustic and aerodynamic field.<sup>9,10</sup> Sound generated by a turbulent flow in the presence of a flexible boundary further complicates the direct computation of sound because of the very stringent requirement in the

computation of the acoustic field, the flow field, and the flow-induced vibration of the flexible boundary. There have been studies concerning the noise radiated from plate vibration driven by a turbulent flow by assuming a certain turbulence spectrum (for instance, Davies,<sup>11</sup> Wu and Maestrello,<sup>12</sup> and Dowell<sup>13</sup>). However, such assumption tends to ignore the important coupling among the flow, the acoustic field, and the plate. Also, the underlying sound generation mechanisms have not been discussed.

Real turbulence is also difficult to handle theoretically, making the study of aerodynamic sound generation mechanisms difficult. Therefore vortices, though they are drastic simplifications of the turbulent flow, are often adopted to get insights into the sound generation process. Crighton<sup>14</sup> used this vortex analogy to get insight into the radiation of the edge noise. More examples can be found in Howe,<sup>15</sup> Leung and So,<sup>16</sup> and Tang and Lau.<sup>17</sup> The recent work of Tang *et al.*<sup>18</sup> shows the presence of significant dipole and monopole radiation when a vortex moves over a flexible membrane in the absence of a mean flow. The former is due to the transverse motion of the vortex, implying that similar dipole radiation will be produced by the turbulent eddies inside a turbulent flow when they interact with a flexible boundary.

The present investigation is focused on the aeroacoustics when a vortex interacts with a finite length flexible boundary backed by an airtight cavity in the presence of a low Mach number mean flow. The setup is analogous to that of the “drumlike” silencing device of Huang.<sup>8</sup> It is hoped that the results of the present study can provide information on the self-noise of such device in a practical flow duct and to enhance fundamental understanding of aeroacoustics.

## II. THEORETICAL MODEL

The turbulent flow inside a practical duct is of high Reynolds number but low Mach number. The effect of viscosity is therefore of second importance in the present study.<sup>19</sup> Fig-

<sup>a)</sup>Author to whom correspondence should be addressed; electronic mail: besktang@polyu.edu.hk

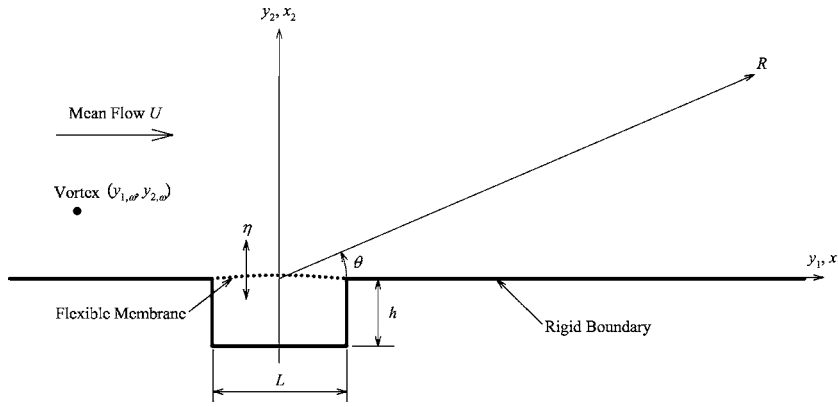


FIG. 1. Schematic of the present theoretical model.

Figure 1 illustrates the schematic of the present study. An inviscid vortex with circulation  $\Gamma$  and initial height  $d$  is chosen. It moves toward the finite length flexible membrane backed by a cavity of depth  $h$  in the presence of a mean parallel flow of velocity  $U$ . This flow extends to the far field. The mechanical properties of the membrane are characterized by the tension per unit spanwise length  $T$ , the mass density  $M_m$ , and the damping factor  $D$  as in Huang<sup>8</sup> and Tang *et al.*<sup>18</sup> In the foregoing discussion,  $\mathbf{y}$  and  $\mathbf{x}$  denote positions in the near and far fields, respectively, with origin at the middle of the membrane.

### A. Vortex dynamics and membrane vibration

Since the vibration displacement magnitude of the membrane is very small when compared to  $d$  ( $< 1\%$  in the present study), the membrane is modeled as a rigid surface with a time varying velocity perturbation  $v$  in the present study as in Tang *et al.*<sup>16</sup> The velocity of the vortex  $v_\omega$  at the position  $(y_{1,\omega}, y_{2,\omega})$  is

$$v_\omega = \left( U + \frac{\Gamma}{4\pi y_{2,\omega}} \right) \hat{y}_1 + \frac{\hat{y}_1}{\pi} \int_{-L/2}^{L/2} \frac{v(y_{1,\omega} - y_1)}{(y_{1,\omega} - y_1)^2 + y_{2,\omega}^2} dy_1 + \frac{\hat{y}_2}{\pi} \int_{-L/2}^{L/2} \frac{v y_{2,\omega}}{(y_{1,\omega} - y_1)^2 + y_{2,\omega}^2} dy_2, \quad (1)$$

where the last two terms on the right-hand side of Eq. (1) represent the fluid velocity induced by the vibrating flexible boundary at the position of the vortex, which are obtained by potential theory.<sup>20</sup>

The unsteady vortex motion induces fluid pressure fluctuation over the flexible membrane and thus modulates  $v(=\partial\eta/\partial\tau)$ . The governing equation for the membrane vibration is

$$M_m \frac{\partial^2 \eta}{\partial \tau^2} = T \frac{\partial^2 \eta}{\partial y_1^2} - D \frac{\partial \eta}{\partial \tau} - \Delta p, \quad (2)$$

where  $\Delta p$  is the fluid pressure differential across the membrane. The fluid pressure above the membrane,  $p^+$ , can be obtained from the linearized Bernoulli relationship<sup>21</sup>

$$p^+ = -\rho_0 \left( \frac{\partial \phi}{\partial \tau} + U \frac{\partial \phi}{\partial y_1} \right), \quad (3)$$

where  $\rho_0$  is the fluid density and  $\phi$  the incompressible velocity potential on the upper surface of the membrane:

$$\phi = -\frac{\Gamma}{2\pi} \tan^{-1} \left[ \frac{2y_{2,\omega}(y_1 - y_{1,\omega})}{(y_1 - y_{1,\omega})^2 + (\eta^2 - y_{2,\omega}^2)} \right] + \frac{1}{\pi} \int_{-L/2}^{L/2} \frac{\partial \eta'}{\partial \tau} \log \sqrt{(y_1 - y_1')^2 + (\eta - \eta')^2} dy_1' + U y_1, \quad (4)$$

where the prime denotes a quantity along the membrane. The second term on the right-hand side of Eq. (4) can be regarded as a kind of fluid loading,<sup>22</sup> but can be neglected in the present study as long as  $\eta$  is kept small and the vibration frequency is low. While fluid compressibility is not important above the membrane because of the much stronger hydrodynamic pressure resulting from the unsteady vortex motions and membrane vibrations, it is the only mean which creates pressure fluctuations inside the cavity. It will be shown later that the frequency of the membrane vibration is much lower than the first eigenmode frequency of the cavity, so that the fluid pressure inside the cavity can be assumed to be uniform. One can then write

$$p^- = c^2 \Delta \rho = -\frac{c^2 \rho_0}{Lh} \int_{-L/2}^{L/2} \eta dy_1 \quad (5)$$

and  $\Delta p = p^+ - p^-$ . The motions of the vortex and the membrane can be obtained by time integration of Eqs. (1) and (2) using a fourth-order Runge-Kutta procedure.

### B. Acoustic far field

At a point  $\mathbf{X}$  fixed in the fluid and thus moving with the local fluid velocity in the far field, the quadrupole in the solutions of acoustic analogy<sup>1,2</sup> at low Mach number  $M$  ( $M = U/c$ , where  $c$  is the ambient speed of sound) can be ignored so that the acoustic pressure at  $\mathbf{X}$  is

$$p(\mathbf{X}, t) = \frac{\rho}{2\pi} \left[ \frac{\partial}{\partial t} \int_S \frac{\mathbf{u} \cdot \mathbf{n}}{r} dS(\mathbf{Y}) - \nabla_{\mathbf{x}} \cdot \int_S (\rho \mathbf{u}(\mathbf{u} \cdot \mathbf{n}) + p \mathbf{n}) \frac{dS(\mathbf{Y})}{r} \right], \quad (6)$$

where  $\mathbf{Y}$  is a point in the near flow field,  $r = |\mathbf{X} - \mathbf{Y}|$ ,  $\mathbf{n}$  is the outward normal of the surface  $S$ , and the integrands are evaluated at the retarded time  $t - r/c$ . The first term on the right-hand side of Eq. (6) is due to the membrane vibration. Following the result of Ffowcs Williams and Lovely,<sup>6</sup> which

is for a compact point source, this term can be evaluated by an integration along the spanwise direction of the system:

$$p_{\text{vib}}(\mathbf{X}, t) = \frac{\rho}{2\pi} \int_{-\infty}^{\infty} \frac{1}{|\mathbf{X} - \mathbf{Y}|(1 + M \cos \theta')^3} \frac{\partial^2}{\partial \tau^2} \eta(\mathbf{y}, t - |\mathbf{X} - \mathbf{Y}|/c) dy_1 dy_3 + O(M^2), \quad (7)$$

and

$$\cos \theta' = \hat{\mathbf{Y}}_1 \cdot \frac{\mathbf{X} - \mathbf{Y}}{|\mathbf{X} - \mathbf{Y}|} = \frac{X_1 - Y_1}{r}. \quad (8)$$

The second term on the right-hand side of Eq. (6) represents the sound radiation due to the fluctuating forces and rate of momentum transfer at the vibrating membrane boundary, which must equal the force that gives rise to the unsteady motions of the vortex.<sup>21</sup> The force per unit spanwise length,  $\mathbf{F}$ , acting on the fluid in the present two-dimensional system is thus

$$\mathbf{F} = \int_{-L/2}^{L/2} [\rho \mathbf{u}(\mathbf{u} \cdot \mathbf{n}) + p \mathbf{n}] dy_1 = \rho \Gamma \hat{\mathbf{y}}_3 \times (\mathbf{v}_\omega - \mathbf{v}'_\omega), \quad (9)$$

where  $\mathbf{v}'_\omega$  is the velocity of the image vortex.<sup>23</sup> The far field acoustic contribution from this force is

$$p_{\text{force}}(\mathbf{X}, t) = \frac{\rho}{2\pi c} \int_{-\infty}^{\infty} \frac{(\mathbf{X} - \mathbf{Y})}{|\mathbf{X} - \mathbf{Y}|^2(1 + M \cos \theta')^2} \cdot \frac{\partial}{\partial \tau} \mathbf{F}(\mathbf{y}, t - |\mathbf{X} - \mathbf{Y}|/c) dy_3 + O(M^2). \quad (10)$$

As shown by Ffowcs Williams and Hawkins,<sup>24</sup> the integration along the direction  $y_3$  in Eqs. (8) and (10) can be transformed into a time integration which is dominated by the contributions at  $y_3 \rightarrow 0$ . Therefore,

$$p(\mathbf{X}, t) = \frac{\rho}{\pi \sqrt{2R}(1 + M \cos \theta)^2} \left\{ \int_{-\infty}^{t-|\mathbf{X}|/c} \frac{1}{\sqrt{c(t-\tau)-R}} \times \left[ \frac{1}{(1 + M \cos \theta)} \int_{-L/2}^{L/2} \frac{\partial^2 \eta}{\partial \tau^2} dy_1 + \frac{1}{c} \frac{\partial \mathbf{F}}{\partial \tau} \cdot \frac{\mathbf{X}}{|\mathbf{X}|} \right] d\tau \right\}, \quad (11)$$

where  $R = \sqrt{(X_1 - Y_1)^2 + (X_2 - Y_2)^2} = \sqrt{(x_1 - y_1)^2 + (x_2 - y_2)^2}$  and  $\cos \theta = (x_1 - y_1)/R$ . The line integral in Eq. (11) can be performed by a substitution depicted in Tang and Ko.<sup>25</sup>

### III. RESULTS AND DISCUSSIONS

In the present study, the mean flow is introduced abruptly into the system which is initially at rest. This results in an initial swelling of the membrane because of the mean fluid pressure difference between the near flow field and the cavity. The vortex path deflects away from the rigid plane at the same time. The air pressure on both sides of the membrane is not equalized initially in the present study because the flow speed inside a practical ventilation duct can vary according to the ventilation requirement and/or heating/

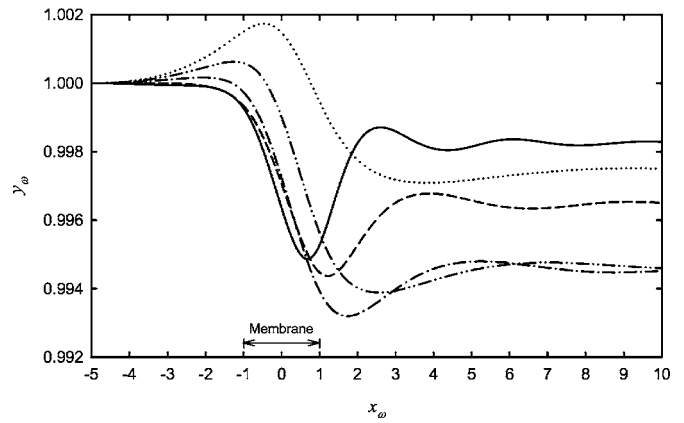


FIG. 2. Effects of mean flow velocity on vortex paths at  $c_m=1$ . (—)  $U=0$ ; (---)  $U=0.5$ ; (-.-)  $U=1$ ; (---)  $U=1.5$ ; and (···)  $U=2$ .

cooling load inside a centrally ventilated building automatically within operation hours. Therefore, the associated equalization of air pressure will require some kind of control system to be in place. Also, the flow is driven by a fan which should be started up from rest.

All length scales in the present study are normalized by  $d$  and all velocities by the initial vortex speed due to self-induction, which is  $U_i = \Gamma/4\pi d$ . The tension per unit length,  $T$ , the damping coefficient  $D$ , and the mass density of the membrane  $M_m$  are normalized by  $\rho U_i^2 d$ ,  $\rho U_i$ , and  $\rho d$ , respectively. Since the structural damping within the membrane is in practice very weak, its effects are not discussed here. In the literature, for instance Frendi *et al.*,<sup>26</sup>  $D$  varies between 0.5 and 1 which refers to very weak damping condition.<sup>18</sup>  $D$  is fixed at unity throughout the present investigation. The *in vacuo* wave speed along the membrane is  $c_m = \sqrt{T/M_m}$ , which is again normalized by  $U_i$ . To ensure a low Mach number condition,  $U_i$  is fixed at 0.1c. Huang<sup>8</sup> shows using a real material example that  $c_m$  can be set to 0.1c and thus the present range for  $c_m$  is chosen to be around 1 (maximum 2).

In reality, the vortex circulation and the mean flow speed are two related quantities as discussed by Lau and Tang<sup>27</sup> with a formula given in Saffman.<sup>28</sup> The general conclusion is that  $U \sim 1$ . However, since the formula in Saffman<sup>28</sup> is a general approximation, a range of  $U$  should be allowed in the present study. More detailed discussions on the relationship between the mean flow and the vortex circulation can be found in Lau and Tang.<sup>27</sup>

The magnitude of the membrane deflection is kept below 1% of  $d$  (and  $h=1$ ) throughout the present study. Given the very small degree of membrane stretching (maximum 0.5%) and that the membrane should be stretched to a great extent to maintain the tension, the effect of the tension variation should be insignificant. Such assumption was basically justified by the experiments of Choy and Huang<sup>29</sup> within engineering tolerance.

#### A. Vortex paths and membrane vibration

The flight paths of the vortex under different mean flow  $U$  with  $c_m=1$  are shown in Fig. 2. The vortex moves toward the membrane due to the finite impedance of the latter.<sup>30</sup> The maximum transverse deviation from the original vortex po-

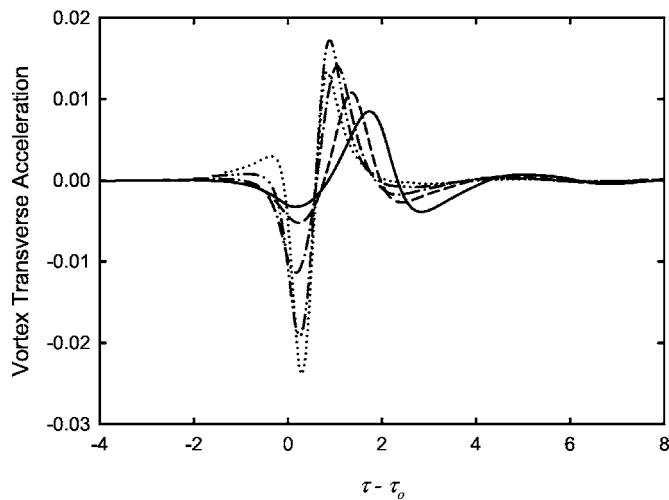


FIG. 3. Time variations of vortex transverse accelerations for  $c_m=1$ . Legends: same as those for Fig. 2.

sition increases with  $U$  for  $U \leq 1$  and decreases upon further increase of  $U$ . The mean flow introduces a mean pressure difference on the two sides of the membrane. This tends to create an initial swelling of the membrane and thus the vortex paths, especially for strong  $U$ . The maximum  $y_{2,\omega}$  increases monotonically with  $U$  because of the mean pressure difference induced by  $U$  mentioned before. This maximum is attained before the vortex traverses over the centerline of the membrane ( $y_1=0$ ).

The relatively strong vortex accelerations at the instants the vortex reaches the leading and trailing edges of the membrane shown in Fig. 3 suggest significant vortex dipole sound is radiated only when the vortex is moving over the membrane.  $\tau_0$  denotes the instant the vortex is directly above the leading edge of the membrane. The instant the vortex reaches the trailing edge of the membrane is roughly  $\tau_0 + 2/(U+U_i)$ . The magnitude of the earlier acceleration peak increases with  $U$ , but the later one increases with  $U$  only up to  $U \sim 1.5$

where the upward movement of the vortex is less affected by the restoring force of the membrane and the rigid edge at  $y_1=-1$  as such high  $U$  tends to wash the vortex faster downstream, reducing the interaction time between the vortex and the membrane system. One can notice this also from Fig. 2, which illustrates that the vortex attains its minimum transverse position at increased  $y_1$  as  $U$  increases. At  $U=2$ , this position is reached even when the vortex is downstream of the membrane.

The time variations of the membrane vibration velocity ( $\partial\eta/\partial\tau$ ) at  $U=1.25$  and 2 with  $c_m=1$  are shown in Figs. 4(a) and 4(b), respectively. Maximum membrane/vortex path deflection occurs at  $U \sim 1$  to 1.25. The corresponding patterns for  $U < 1.25$  resemble that of Fig. 4(a) with smaller magnitudes and thus are not presented. At  $U=2$ , the macroscopic vibration velocity pattern still looks similar to that at  $U=1.25$ , but it has become irregular with steeper variations. One can notice from Fig. 4 that membrane vibration frequency is very low. The highest vibration frequency in the present study occurs at  $U=3$ ,  $c_m=2$  which equals  $0.518d/U_i$  and is roughly one-fifth of the lowest cavity eigenmode frequency ( $5U_i/L$ ). The recent results of Huang<sup>31</sup> confirm the validity of the present assumption of uniform air pressure inside the cavity at such low frequency ratio [Eq. (5)].

An increase in  $c_m$  does not bring about very significant change in the vortex paths as shown in Fig. 5(a). However, at a high  $c_m=2$ , one can observe a minor dip in the minimum  $y_\omega$  at  $U \sim 0.5$  but the lowest  $y_\omega$  appears at  $2.5 < U < 3$ . The relatively strong membrane tension in this case limits the upward motion of the membrane due to the mean fluid pressure difference under the stronger mean flow. Computation is stopped at  $U=3$ , which corresponds to a Mach number  $U/c$  of 0.3; a value close to the limit of the acoustic analogy. Figure 5(b) illustrates the vortex path at  $c_m=1/\sqrt{2}$ . The weaker tension allows a larger upward stretch of the membrane. The lowest  $y_\omega$  in this case appears at a  $U$  less than  $c_m$ .

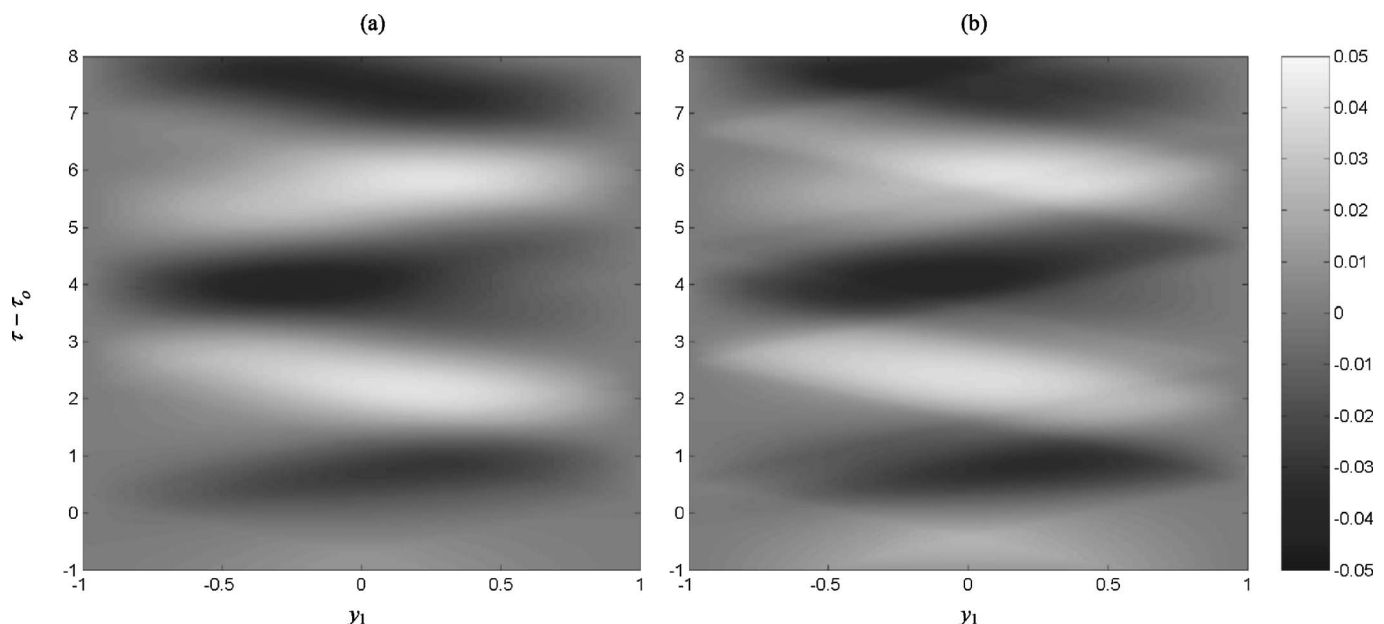


FIG. 4. Membrane vibration velocity patterns for  $c_m=1$ . (a)  $U=1.25$  and (b)  $U=2$ .



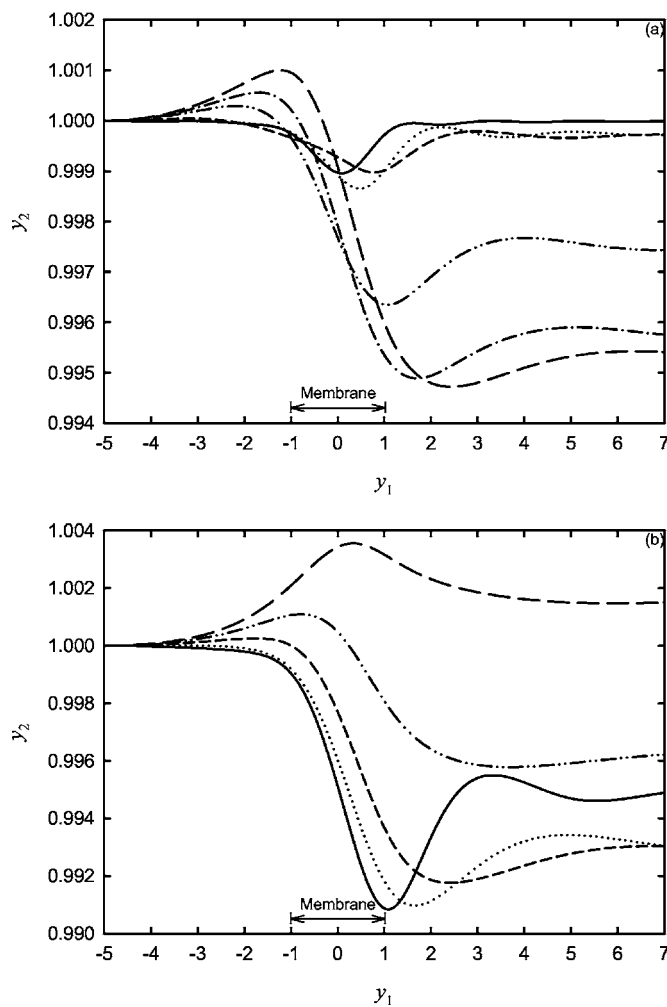


FIG. 5. Vortex paths at different  $c_m$ . (a)  $c_m=2$  and (b)  $c_m=1/\sqrt{2}$ .

The pattern of the vortex path variation with  $U$  shown in Fig. 5(b) is similar to those at  $U > c_m$  presented in Figs. 2 and 5(a).

The results shown in Fig. 6 suggest that the lowest  $y_{2,\omega}$  is found at  $U+0.5U_i \approx 1.63c_m$  for  $c_m \geq 1$ . There is also a

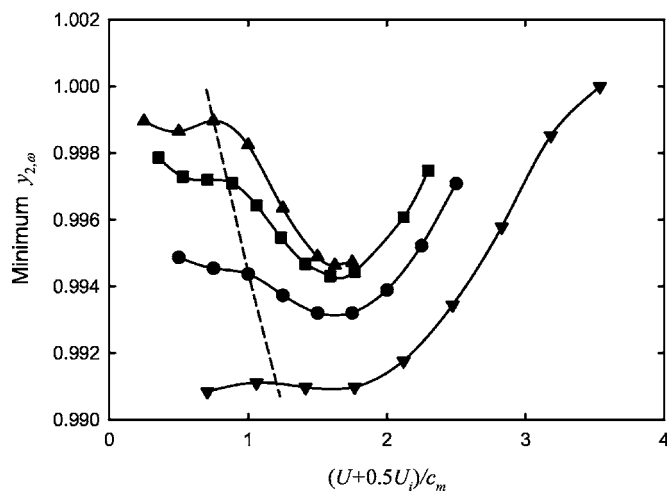


FIG. 6. Relationship between minimum vortex height and flow speed. (---) Approximate location of  $U/c_m=0.5$ ; ( $\nabla$ )  $c_m=1/\sqrt{2}$ ; ( $\bullet$ )  $c_m=1$ ; ( $\blacksquare$ )  $c_m=\sqrt{2}$ ; and ( $\blacktriangle$ )  $c_m=2$ .

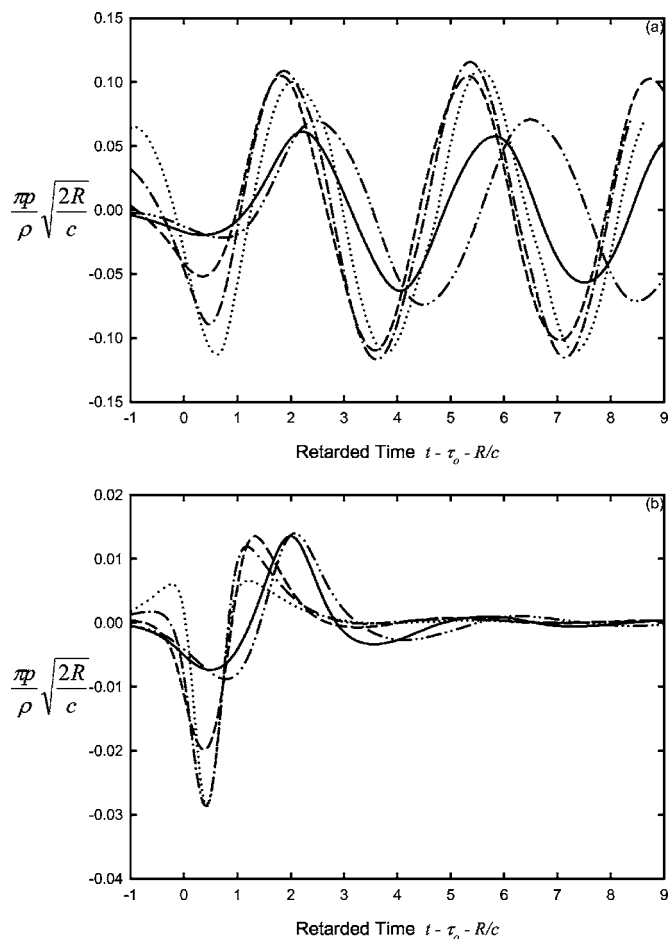


FIG. 7. Time variations of sound field strengths for  $c_m=1$ . (a) Monopole and (b) dipole. (—)  $U=0$ ; (---)  $U=1$ ; (-·-)  $U=1.5$ ; (···)  $U=2$ ; (---)  $U=0$  (without cavity)—Ref. 16.

local minimum at a similar location for  $c_m=1/\sqrt{2}$ . Without the mean flow and the cavity, the lowest  $y_{2,\omega}$  decreases monotonically with increasing  $c_m$ .<sup>16</sup> For small  $U$ , the variation of the lowest  $y_{2,\omega}$  is not significant, but it drops for  $U/c_m > 0.5$  before a minimum is reached with a rate which increases with increasing  $c_m$ . The increase in the fluid pressure due to the vortex motion depends on the vortex speed and thus is partially related to  $U$ , but the latter reduces the mean fluid pressure above the membrane relative to that within the cavity counteracting the former effect. The effect of the mean pressure difference predominates at  $U+0.5U_i \approx 1.63c_m$ . The value 1.63 is believed to be associated with the volume of the cavity. It is left to further investigation.

## B. The acoustic far field

The far field acoustic pressure fluctuations for  $c_m=1$  are presented in Fig. 7 with the Doppler factor  $(1+M \cos \theta)$  excluded. These pressure fluctuations are normalized in the same way as in Tang *et al.*<sup>18</sup> The corresponding results of Tang *et al.*<sup>18</sup> are included for the sake of easy comparison. The monopole radiations are shown in Fig. 7(a). The presence of the cavity below the membrane weakens the monopole radiation but increases the frequency of the radiation. The latter is expected as the cavity adds to the stiffness of the membrane. The increase in  $U$  produces a louder initial sound

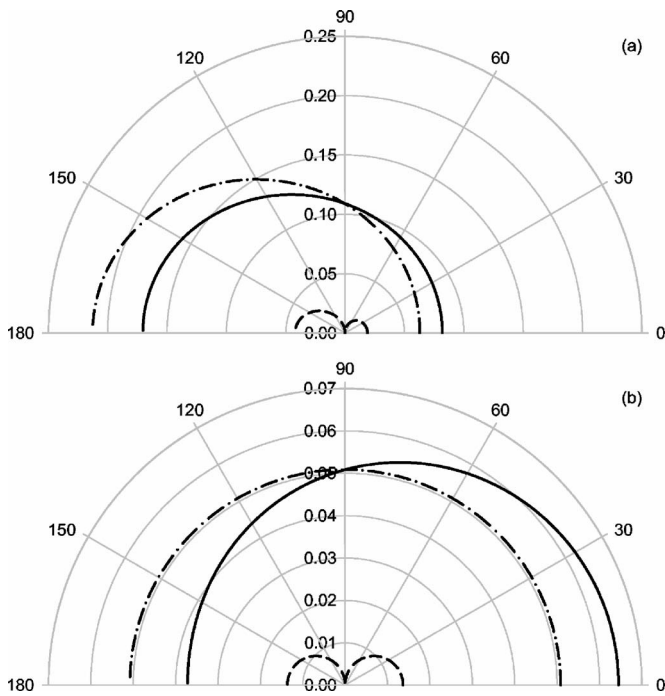


FIG. 8. Directivity of overall sound radiation at instants of strongest dipole radiation. (a)  $U=2$  and (b)  $U=0$ .  $c_m=1$ . (—) Overall radiation; (---) monopole; and (- - -) dipole.

radiation. However, the corresponding sound amplitude peaks at around  $U \sim 1.5$ , probably due to the more dominant effect of the mean pressure difference between the flow and the cavity.

The corresponding dipole strengths are shown in Fig. 7(b). One can observe the eventual gain in dominance of the negative trough as  $U$  increases. The magnitude of the positive peak of this dipole time variation does not depend much on  $U$  for  $U < 1$ . Though the Doppler factor tends to attenuate more for the monopole radiation for  $\theta < \pi/2$  as indicated in Eq. (11), the magnitude of the monopole remains more than three times that of the dipole at  $\theta=0$  for  $U=2$  ( $M=0.2$ ). The corresponding ratio is  $\sim 3.7$  in the absence of the mean flow. The increase in  $U$  shortens the period of active dipole radiation as expected.

Figure 7 indicates that the monopole and the dipole are nearly in phase (of the same sign) when the vortex is traversing in the proximity of the membrane for  $0 \leq t - \tau_0 - R/c \leq 1$ . Therefore, these two sound fields will be counteracting with each other for  $\theta > \pi/2$ . Figure 8(a) illustrates the directivity of sound radiation at  $t - \tau_0 - R/c = 0.5$  for  $U=2$ ,  $c_m=1$ , which corresponds to the instant of strongest dipole radiation [Fig. 7(b)]. The combined action of the two sound fields tends to reduce the effect of the Doppler factor. The corresponding sound fields in the absence of the mean flow at the instant of strongest dipole radiation are presented in Fig. 8(b). Without the mean flow, a downstream biased radiation as in Tang *et al.*<sup>18</sup> is observed. The results with  $U=1$  ( $M=0.1$ ) still show a slightly downstream biased overall sound radiation (not presented here). Outside the active dipole radiation period, the monopole results in an upstream biased radiation. One can also notice the very strong convective amplification of the monopole in the presence of the mean

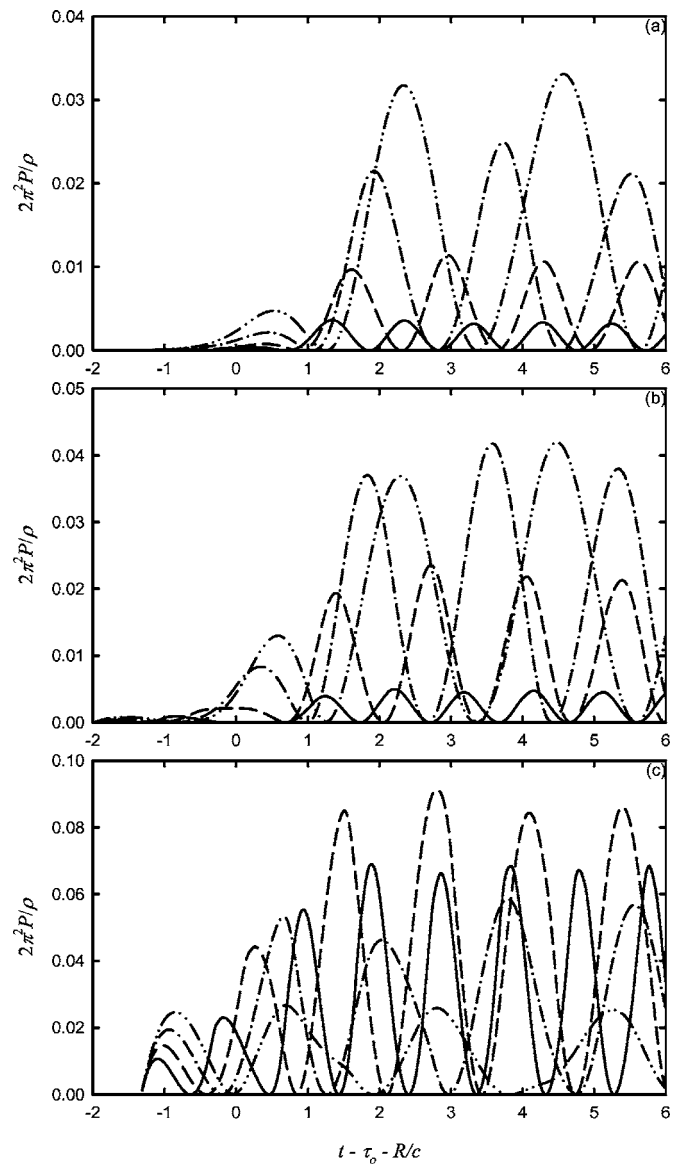


FIG. 9. Time variation of acoustic power radiation. (a)  $U=0.5$ ; (b)  $U=1$ ; and (c)  $U=2$ . (—)  $c_m=2$ ; (---)  $c_m=\sqrt{2}$ ; (- - -)  $c_m=1$ ; and (- - -)  $c_m=1/\sqrt{2}$ .

flow, such that the overall sound power radiation is dominated by this monopole, which results from the vortex induced vibration of the membrane. Similar data variations as in Figs. 7 and 8 are observed at other values of  $c_m$  and thus the corresponding results are not presented.

The acoustic power radiated per unit spanwise length of the membrane,  $P$ , is summarized in Fig. 9.  $P$  is obtained by integrating  $p^2(\mathbf{X}, t)/\rho c$  [Eq. (11)] over a distant cylindrical surface fixed in space with radius  $|\mathbf{X}|$ . For  $U=0.5$ , the acoustic power increases with decreasing  $c_m$  [Fig. 9(a)], but the trend is reversing gradually as  $U$  increases as illustrated in Figs. 9(b) and 9(c). For  $c_m \geq 1$ , the acoustic power increases with increasing  $U$  but the rate of increase depends on  $c_m$ . For  $c_m=1$ , the increase in the acoustic power radiated due to the increase of  $U$  toward 2 is limited. The rate of acoustic power increase is impressive for  $c_m=2$  when  $U$  increases beyond 1.

The variation of the radiated acoustic power magnitude with  $U$  is nearly negligible for  $c_m=1/\sqrt{2}$  and a reduction is

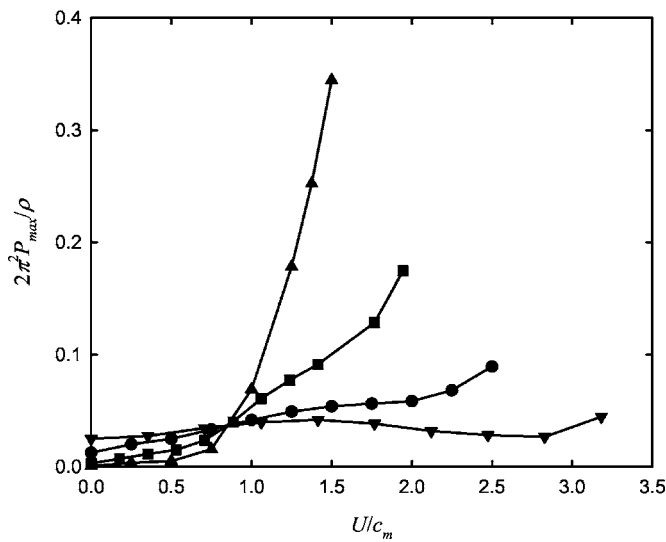


FIG. 10. Maximum radiated acoustic power under different combinations of  $U$  and  $c_m$ . (▼)  $c_m = 1/\sqrt{2}$ ; (●)  $c_m = 1$ ; (■)  $c_m = \sqrt{2}$ ; and (▲)  $c_m = 2$ .

observed as  $U$  increases toward 2. Both the membrane vibration and the vortex acceleration are significantly weakened at high  $U$  because of the large mean fluid pressure difference between the flow and the cavity. Such weakening is more significant than the amplification of the monopole and the dipole in the presence of the mean flow. There is thus a higher chance of occurrence of a downstream biased radiation at small  $c_m$ .

Figure 10 illustrates in detail the maximum acoustic power radiated,  $P_{\max}$ , under the combined effects of  $U$  and  $c_m$ .  $P_{\max}$  increases with decreasing  $c_m$  for  $U/c_m < 0.8$ , but the opposite is found otherwise. This  $U/c_m \sim 0.8$  is also the location where the negative trough of the dipole strength starts to be more dominant in the overall dipole power radiation. For  $U/c_m \leq \sqrt{2}$ , the rate of increase of  $P_{\max}$  tends to decrease with increasing  $U/c_m$  before a maximum or an inflexion point is found on the curves. For a weak membrane-cavity system, a reduction in  $P_{\max}$  is observed for a range of  $U/c_m$ , but this power increases again when  $U$  is kept increasing toward 3 ( $M=0.3$ ), which is the upper limit for the acoustic analogy. The later rise in  $P_{\max}$  is due to the strong mean fluid pressure difference between the flow and the cavity leading to the very early but high membrane and vortex upward accelerations (not shown here). It is believed that this phenomenon occurs even for membrane of high wave speed.

It is found that the vortex dipole in the presence of the mean flow has adverse effects on the overall acoustic power radiation (Fig. 11). Apart from the case for  $U=0$  where the vortex dipole adds to the overall radiation, this dipole tends to counteract with the effect of the convective amplification in the presence of the mean flow. Also, the stronger the mean flow, the stronger such cancellation will be regardless of the value of  $c_m$ . The contribution from the dipole is insignificant for  $U=0$ ,  $c_m=2$  as shown in Fig. 11(b).

#### IV. CONCLUSIONS

The effects of a low Mach number mean flow on the sound radiated by the unsteady motion of a vortex moving in

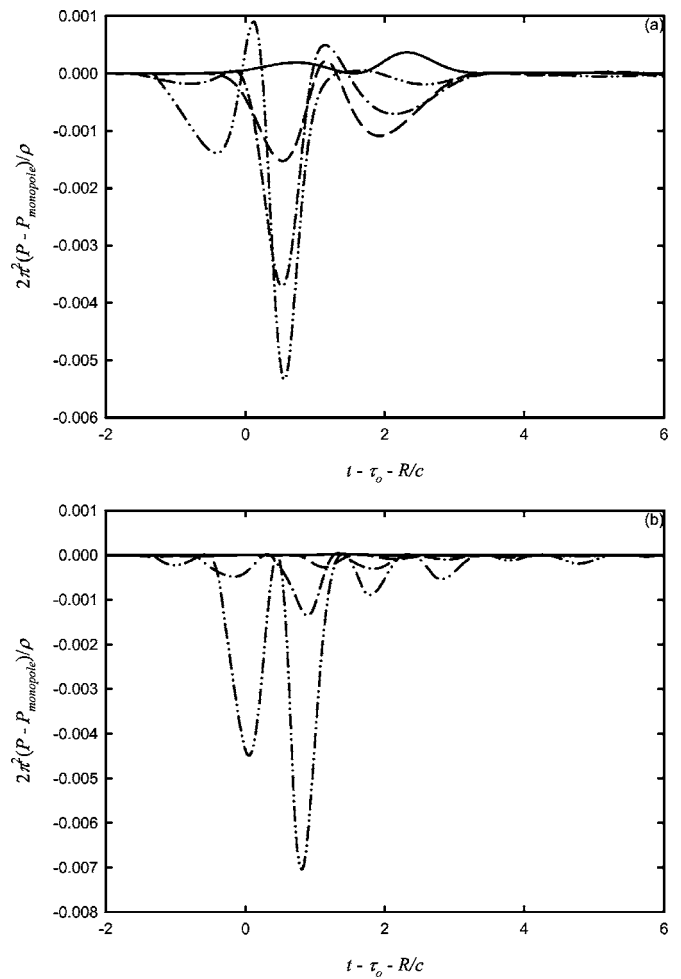


FIG. 11. Contributions from vortex dipole to acoustic power radiation. (a)  $c_m = 1/\sqrt{2}$  and (b)  $c_m = 2$ . (—)  $U=0$ ; (---)  $U=1$ ; (-·-)  $U=1.5$ ; and (---)  $U=2$ .

the proximity of a finite length flexible membrane backed by an airtight cavity on an otherwise rigid plane are investigated in detail theoretically in the present study.

The vortex moves toward the flexible membrane transversely as it propagates over the leading edge of the membrane and then moves upwards as it traverses over the membrane trailing edge when the mean flow is not high. The mean flow results in a higher vortex longitudinal speed which increases the fluid pressure acting on the membrane. However, the presence of the mean flow and the cavity also gives rise to a mean fluid pressure difference between the two sides of the membrane, which tends to reduce the vibration magnitude of the membrane when the mean flow becomes high, especially for a weak membrane. The former factor is dominant in low mean flow speed cases, but the latter takes over when the mean flow exceeds a certain threshold depending on the wave speed of the membrane. The introduction of the cavity in general reduces the magnitude of the vortex induced membrane vibration and thus weakens the sound radiation. However, it is found that such effect does not vary monotonically with the flow speed because of the two counteracting forces stated earlier.

The vortex motion generates a dipole which propagates to the far field together with the monopole created by the



membrane vibration. The former is usually an order weaker than the latter. These sound fields counteract with each other in the upstream radiation directions. The mean flow results in amplifications of both sound fields, but in general, the overall effect is that the monopole receives a higher amplification due to the convective effect and the stronger vibration of the membrane. The dipole is only important in the period when the vortex is in close proximity of the membrane. Under some circumstances, the dipole strength may be strong enough to cause a fluctuation in the overall radiation directivity. However, the increase in the mean flow speed does not strengthen the overall acoustic power radiation when the membrane system is weak compared to the mean flow momentum. It is observed that an attenuation of the acoustic power radiation is possible when the mean flow speed is high compared to the membrane wave speed where the weakening of the membrane vibration cannot be compensated by the amplification resulting from the mean flow in the presence of the counteracting vortex dipole.

## ACKNOWLEDGMENT

Funding support under Grant No. PolyU1/02C from the Research Grants Council of the Government of the HKSAR is gratefully acknowledged.

- <sup>1</sup>M. J. Lighthill, "On sound generated aerodynamically I. General theory," *Proc. R. Soc. London, Ser. A* **211**, 564–587 (1952).
- <sup>2</sup>N. Curle, "The influence of solid boundaries upon aerodynamic sound," *Proc. R. Soc. London, Ser. A* **231**, 505–514 (1955).
- <sup>3</sup>L. L. Beranek, *Noise and Vibration Control, Principles and Applications* (Wiley, New York, 1992).
- <sup>4</sup>L. E. Kinsler, A. R. Frey, A. B. Coppens, and J. V. Sanders, *Fundamentals of Acoustics*, 4th ed. (Wiley, New York, 2000).
- <sup>5</sup>J. E. Ffowcs Williams and D. J. Lovely, "Sound radiation into uniformly flowing fluid by compact surface vibration," *J. Fluid Mech.* **71**, 689–700 (1975).
- <sup>6</sup>A. Dowling, "Convective amplification of real simple sources," *J. Fluid Mech.* **74**, 529–546 (1976).
- <sup>7</sup>M. S. Howe, "Mechanism of sound generation by low Mach number flow over a wall cavity," *J. Sound Vib.* **273**, 103–123 (2004).
- <sup>8</sup>L. Huang, "A theoretical study of duct noise control by flexible panels," *J. Acoust. Soc. Am.* **106**, 1801–1809 (1999).
- <sup>9</sup>M. R. Visbal and D. V. Gaitonde, "Very high-order spatially implicit schemes for computational acoustics on curvilinear meshes," *J. Comput.*

- Acoust.* **9**, 1259–1286 (2001).
- <sup>10</sup>R. C. K. Leung, X. M. Li, and R. M. C. So, "Comparative study of nonreflecting boundary condition for one-step duct aeroacoustic simulation," *AIAA J.* **44**, 664–667 (2006).
- <sup>11</sup>H. G. Davies, "Sound from turbulent boundary layer excited panels," *J. Acoust. Soc. Am.* **49**, 878–889 (1971).
- <sup>12</sup>S. F. Wu and L. Maestrello, "Responses of finite baffled plate to turbulent flow excitations," *AIAA J.* **33**, 13–19 (1995).
- <sup>13</sup>E. H. Dowell, "Radiation from panels as a source of airframe noise," *AIAA J.* **13**, 1529–1530 (1975).
- <sup>14</sup>D. G. Crighton, "Radiation from vortex filament motion near a half-plane," *J. Fluid Mech.* **51**, 357–362 (1972).
- <sup>15</sup>M. S. Howe, *Theory of Vortex Sound* (Cambridge University Press, Cambridge, 2003).
- <sup>16</sup>R. C. K. Leung and R. M. C. So, "Noise generation of blade-vortex resonance," *J. Sound Vib.* **245**, 217–237 (2001).
- <sup>17</sup>S. K. Tang and C. K. Lau, "Vortex sound in the presence of a wedge with inhomogeneous surface flow impedance," *J. Sound Vib.* **281**, 1077–1091 (2005).
- <sup>18</sup>S. K. Tang, R. C. K. Leung, R. M. C. So, and K. M. Lam, "Acoustic radiation by vortex induced flexible wall vibration," *J. Acoust. Soc. Am.* **118**, 2182–2189 (2005).
- <sup>19</sup>D. G. Crighton, "Basic principles of aerodynamic noise generation," *Prog. Aerosp. Sci.* **16**, 31–96 (1975).
- <sup>20</sup>H. R. Vallentine, *Applied Hydrodynamics* (Butterworth, London, 1969).
- <sup>21</sup>N. Peake, "On the unsteady motion of a long fluid-loaded elastic plate with mean flow," *J. Fluid Mech.* **507**, 335–366 (2004).
- <sup>22</sup>P. J. T. Filippi, O. Lagarrigue, and P.-O. Mattei, "Perturbation method for sound radiation by a vibrating plate in a light fluid: Comparison with the exact solution," *J. Sound Vib.* **177**, 259–275 (1994).
- <sup>23</sup>S. K. Tang and J. E. Ffowcs Williams, "Acoustic radiation from a vortex approaching a circular cylinder with surface suction," *Acust. Acta Acust.* **84**, 1007–1013 (1998).
- <sup>24</sup>J. E. Ffowcs Williams and D. L. Hawkings, "Shallow water wave generation by unsteady flow," *J. Fluid Mech.* **31**, 779–788 (1968).
- <sup>25</sup>S. K. Tang and N. W. M. Ko, "Sound generation by interaction of two inviscid two-dimensional vortices," *J. Acoust. Soc. Am.* **102**, 1463–1473 (1997).
- <sup>26</sup>A. Frendi, L. Maestrello, and A. Bayliss, "Coupling between plate vibration and acoustic radiation," *J. Sound Vib.* **177**, 207–226 (1994).
- <sup>27</sup>C. K. Lau and S. K. Tang, "Sound generated by vortices in the presence of a porous half-cylinder mounted on a rigid plane," *J. Acoust. Soc. Am.* **119**, 2084–2095 (2005).
- <sup>28</sup>P. G. Saffman, *Vortex Dynamics* (Cambridge University Press, Cambridge, UK, 1992).
- <sup>29</sup>Y. S. Choy and L. Huang, "Effect of flow on the drumlike silencer," *J. Acoust. Soc. Am.* **118**, 3077–3085 (2005).
- <sup>30</sup>S. K. Tang, "Effects of porous boundaries on the dynamics of an inviscid vortex filament," *Q. J. Mech. Appl. Math.* **54**, 65–84 (2001).
- <sup>31</sup>L. Huang, "Modal analysis of a drumlike silencer," *J. Acoust. Soc. Am.* **112**, 2014–2025 (2002).